Detecting settlement expansion in South Africa using a hyper-temporal SAR change detection approach

W. Kleynhans[a,b,d], B.P. Salmon[b,c], J.C. Olivier[c]

[a] *Department of Electrical, Electronic and Computer Engineering, University of Pretoria, South Africa.*
[b] *Remote Sensing Research Unit, Meraka Institute, CSIR, South Africa.*
[c] *School of Engineering, University of Tasmania, Australia*
[d] *VizCenter, San Diego State University, USA.*

Abstract

Recent times have seen a significant increase in the amount of readily available SAR data, with many current and historic SAR data holdings now adopting an open distribution policy. As more regular SAR observations are becoming available, the use of a hyper-temporal SAR change detection framework (utilizing a stack of potentially hundreds of SAR images) is now becoming significantly more feasible. A relevant use case is the detection of new informal settlements in South Africa. Here, hyper-temporal change detection has been shown to be very effective but has been limited to coarse resolution optical satellite imagery only. In particular, it has been found that for optical data the Temporal Autocorrelation Change Detection (TACD) method is able to effectively detect the formation of new informal settlements using hyper-temporal MODIS time-series data. In this paper, the TACD is modified for the use of coarse resolution hyper-temporal SAR data for the detection of new informal settlements. It is shown that by using a hyper-temporal approach to detecting these new informal settlements, a higher overall accuracy was achievable when compared to standard bi-temporal change detection. A dataset of ENVISAT Advanced Synthetic Aperture Radar images over the study area was used to create a hyper-temporal time-series of backscatter values for each of the pixels in the study area. It was found that the proposed method achieved change detection accuracies of 87% at a false alarm rate of less than 1% with bi-temporal SAR change detection achieving

Email address: wkleynhans@csir.co.za (W. Kleynhans)

a change detection accuracy of 70% at an approximate 1% false alarm rate.

Keywords: change detection, SAR, time-series, hyper-temporal, settlements

1. Introduction

SAR data are becoming increasingly easier to come by as many current and historic SAR data holdings now adopting an open distribution policy. An example of this is historic ENVISAT Advanced Synthetic Aperture Radar (ASAR) and Sentinel-1 data holdings . The Sentinel-1 satellite, for example, is potentially able to map the global landmasses in the Interferometric Wide swath mode once every 12 days and this reduces to a 6 day exact repeat cycle at the equator when both Sentinels are operational [1]. As more regular SAR observations are becoming available from new and historic SAR satellites, the use of a hyper-temporal SAR change detection framework (utilizing a stack of potentially hundreds of SAR images) is now becoming significantly more feasible [2]. A relevant use case is the detection of new informal settlements in South Africa which is one of the most pervasive forms of land-cover change in many developing countries. [3] These new developments are mostly driven by human migration and socio economic factors that are constantly changing across the African continent and often leads to settlements occurring informally in areas that were previously covered by natural vegetation.

Detailed mapping of settlements are usually done by analysts digitizing features from aerial or high resolution satellite images. These features are then utilized to support spatial planning and need to be updated regularly (at least every two years). Updating maps over large areas using manual digitizing is slow and costly and many agencies, especially in developing countries are constrained due to finite resources which results in feature datasets being outdated, while only a small percentage of the area actually experienced change. Methods that can rapidly indicate areas having a high probability of change is thus very valuable to an analyst as this can be used to direct their attention to high probability change areas for further evaluation using, for example, higher resolution imagery of the area. By using such a targeted approach, an increase in mapping efficiency of up to ten times has been observed compared to a complete re-extraction [4].

In this paper we therefore focus on the development of automated change detection methods based on hyper-temporal satellite imagery to improve the productivity of detailed mapping efforts. Satellite time series data has proven to be an effective data source for change detection [5, 6, 7, 8] and in particular, time series analyses of hyper-temporal optical satellite data has been successfully applied for land cover change detection in South Africa specifically related to the monitoring of human settlement expansion. In [9], a Neural network based post classification change detection approach was used to detect when land cover conversion takes place from natural vegetation to settlement classes. In [10], MODIS time-series data was modeled as a triply modulated cosine function and an Extended Kalman filter was used to track the parameters of the model and declare change based on parameter behavior. In [11], the use of Page's cumulative sum (CUSUM) test was proposed as a method to detect new settlement. An autocorrelation function (ACF) change detection method was recently shown to detect the development of new human settlements in South Africa [3]. This method uses MODIS time-series data, which have previously been shown to be separable (distinguishable) for the natural vegetation and settlement land cover classes considered in this study [12]. The method uses the ACF of a MODIS time-series to provide an indication of the level of time-series stationarity (by considering the stability of the time-series mean and variance over time) which is then consequently used as a measure of land cover change.

In the original formulation of the ACF approach [3], a single pixel's entire time-series for a single band (spanning eight years) was used as input. A change metric was then calculated by considering the properties of the ACF of the time-series. When the resulting change index was compared to a threshold value, a per-pixel based change alarm resulted. In this paper the ACF approach is extended for the use of hyper temporal Synthetic Aperture Radar (SAR) as input as opposed to optical time-series data to produce a change alarm. SAR has been shown in previous studies to be useful in the detection of human settlements [13, 14, 15, 16] but these studies focused mostly on the use of single image processing as opposed to hyper temporal analysis. In this study, it is postulated that hyper-temporal SAR data would be very useful in the detection of new and expanding settlements as SAR reflectance in the temporal domain would be sensitive to changes from natural vegetation to settlement land cover types. Another important consideration in using SAR over multi spectral optical data, is that the detection

of settlements in areas that are mostly covered by natural vegetation using hyper-temporal optical data is mostly driven by the change in the vegetation seasonal time-series. In many cases, a large reduction in natural vegetation due to, for example, clear-cutting and vegetation removal would have a similar change in the hyper-temporal profile than the change to settlement and these types of changes would typically result in false alarms. In the case of using hyper-temporal SAR data, the temporal profile, especially with HH polarization will result in significant changes when a change occurs from natural vegetation to settlement due to the formation of man-made structures.

The objective of this paper is to extend on the original formulation of the ACF method to a robust change detection method that utilizes hyper-temporal SAR data as input that is able to detect the formation of new informal settlements in areas that are typically covered by diverse natural vegetation. The detected changes should then be used to alert operators to areas of possible changes which could thereafter be validated, and the necessary maps updated, using high resolution imagery. The reason for using high resolution imagery as a secondary step is not only to validate whether or not change has occurred but also to make sure that digitization error is kept to a minimum when determining change vectors. Importantly, the false alarm rate should be low ($\leq 1\%$) as the area on which the change algorithm is run is large and the validation of a large number of false alarms could be costly and time consuming. The hyper-temporal change detection approach used in this paper is also compared to a standard bi-temporal [17, 18] change detection approach by using imagery pre and post the change event. It was found that using a stack of SAR images and a hyper temporal change detection formulation has a significant increase in the overall accuracy when compared to the bi-temporal approach.

This paper is organized as follows: A description of the data is given in section 2. The methodology section, detailing the adaption of the temporal ACF for SAR data is given in section 3. Results are presented in section 4 followed by concluding remarks in section 6.

2. Data Description

2.1. Study Area

The study area considered in this study was the Gauteng province of South Africa, which is located in northern South Africa as indicated in figure 1. A total area of approximately 17000 km^2 (centered around 26°07′29.62″S, 28°05′40.40″E) was considered. A total of 158 ASAR Wide-Swath HH images with a pixel spacing of approximately 75 m was obtained for the period 2005/01 to 2011/01. A dataset of no-change pixel time-series (n=180) were identified by means of visual interpretation of high resolution Quickbird images in 2011 and 2005 respectively. The 2011 imagery over the study area were compared to that of 2005 and no-change areas were able to be rapidly determined. There were also 180 examples of confirmed settlement developments during the study period that were obtained by means of visual interpretation of high resolution Quickbird images in 2011 and 2005 respectively. All settlements identified in 2011 were referenced back to 2005 and all the new settlements were digitized using the high resolution data and a subsequent change polygon was created. By overlaying this change polygon with the ASAR image, all pixels that had an overlap of at least 70% with the change polygon were included in the change pixel dataset. The no-change dataset was split into a test (n=90) and unseen (n=90) dataset. The test dataset was used to determine the threshold values for both the hyper-temporal and bi-temporal change detection methods and constituted of only no-change examples.

2.2. Data processing

The entire stack of 158 images were radiometrically calibrated by making use of the orbital information associated with each image, each image was also geocoded. Images were selected so that the majority of the study area were covered by each ASAR image. In the event that a specific area was not covered by an image, temporal spline cubic interpolation was used to infer an estimated HH backscatter value for that specific date. It should be noted that on average, time series missing values was below 8% of the total time series. Apart from missing value estimation, no additional spatial or temporal filtering was done. The reason for this was to determine the worse case accuracy of the method based on the addition of all possible data, with the method not being influenced by, for example, the specific spatial or temporal filtering method used. Figure 2 and 3 shows two examples of

Table 1: Summary of data used for this study

Platform	Envisat
Instrument	Advanced Synthetic Aperture Radar
Geometric resolution	± 150m × 150m
Pixel spacing	± 75m × 75m
Incident Angle	15 - 45 °
Polarization	HH
Period	2005/01 to 2011/01
# Observations	158

change and no-change areas respectively. Figure 4 shows how a pixel time-series was generated using the ASAR image stack with figure 5 showing the SAR HH backscatter time-series for the period 2005/01 to 2011/01 of the change (right) and no-change (left) pixel example.

3. Methodology

3.1. Temporal ACF Change detection (TACD) method

The Temporal ACF change detection (TACD) method proposed in [3] was developed specifically for the use of MODIS time-series data and uses a two stage approach. Firstly, the band, lag and threshold selection is done using a simulated change dataset together with a no-change dataset. Second, the aforementioned parameters are used in an unsupervised manner to detect change. Assume that a MODIS time-series is expressed as

$$\mathbf{X} = \{X_n\}_{n=1}^{n=T}, \tag{1}$$

where X_n is the observation from an arbitrary spectral band at time n and T is the number of time-series observations available. The ACF for time-series $\mathbf{X}$ can then be expressed as [3]

$$R(\tau) = \frac{E[(X_n - \mu)(X_{n+\tau} - \mu)]}{\mathrm{var}(\mathbf{X})}, \tag{2}$$

where τ is the time-lag and E denotes the expectation. The mean of $\mathbf{X}$ is given as μ and the variance, which is used for normalization, is defined as

var($\mathbf{X}$). The mean and variance of the time-series of $\mathbf{X}$ in (2) is required to remain constant through time to determine the true ACF of the time-series. The inconsistency of the mean and variance typically associated with a change pixel's non-stationary time-series becomes apparent when analyzing the ACF of the time-series. The change metric was defined in [3] as the temporal correlation at a specific lag (τ) given as

$$R(\tau) = \delta_\tau. \tag{3}$$

Defining a change threshold (δ^*_τ), a change or no-change decision was made as

$$\text{Change} = \begin{cases} \text{true} & \text{if } R(\tau) \geq \delta^*_\tau \\ \text{false} & \text{if } R(\tau) < \delta^*_\tau \end{cases} \tag{4}$$

The value of τ as well the threshold value (δ^*_τ) was determined by using simulated change and no-change datasets after which the resulting parameters were used to run the algorithm in an unsupervised manner for the entire study area [3].

3.2. SAR Temporal ACF (SAR-TACD) method

The TACD framework proposed in [3] was developed and tested specifically for optical data, a new framework for hyper-temporal SAR time-series data, and, more specifically, ASAR WSM HH backscatter hyper-temporal input data is formulated as follows.

Assume that a SAR time-series is expressed as

$$\mathbf{X^{SAR}} = \{X_n^{SAR}\}_{n=1}^{n=T}, \tag{5}$$

where X_n^{SAR} is an HH intensity ASAR observation at time n and N is the number of time-series observations available. The ACF for time-series $\mathbf{X^{SAR}}$ can then be expressed as

$$R^{SAR}(\tau) = \frac{E[(X_n^{SAR} - \mu)(X_{n+\tau}^{SAR} - \mu)]}{\text{var}(\mathbf{X^{SAR}})}, \tag{6}$$

where τ is the time-lag and E denotes the expectation. The mean of $\mathbf{X^{SAR}}$ is given as μ and the variance is given as var($\mathbf{X^{SAR}}$).

In the original formulation, the TACD method used the autocorrelation at a specific lag (τ) as the change metric, and the value of this lag was determined by use of simulated change, in the proposed SAR TACD framework, a more robust process is utilized by computing

$$\delta_k^{SAR} = \sum_{\tau=1}^{k} R^{SAR}(\tau). \tag{7}$$

From (7) it is evident that the new change metric uses a summation of the first k lags of $R^{SAR}(\tau)$. By using the summation, the method is not as sensitive to the selection of a specific value of τ. A change or no-change decision was made by comparing δ_k^{SAR}, which is computed for each pixel in the image, to a threshold value value δ^*

$$\text{Change} = \begin{cases} \text{true} & \text{if } \delta_k^{SAR} \geq \delta^* \\ \text{false} & \text{if } \delta_k^{SAR} < \delta^* \end{cases} \tag{8}$$

3.2.1. Selection of the k parameter

To evaluate how the overall accuracy is affected by the selection of the value of k, an experiment was performed where the overall accuracy was evaluated for a range of k values. For each value of k, the overall accuracy was calculated as

$$O_A^k = \frac{P(C|C) + P(\overline{C}|\overline{C})}{P(C|C) + P(\overline{C}|\overline{C}) + P(C|\overline{C}) + P(\overline{C}|C)} \tag{9}$$

where

$$P(C|C) = \int_{\delta_k^{SAR}=\delta_k^{opt}}^{\delta_k^{SAR}=\infty} p(\delta_k^{SAR}|C), \tag{10}$$

$$P(C|\overline{C}) = \int_{\delta_k^{SAR}=\delta_k^{opt}}^{\delta_k^{SAR}=\infty} p(\delta_k^{SAR}|\overline{C}), \tag{11}$$

$$P(\overline{C}|C) = \int_{\delta_k^{SAR}=0}^{\delta_k^{SAR}=\delta_k^{opt}} p(\delta_k^{SAR}|C), \tag{12}$$

$$P(\overline{C}|\overline{C}) = \int_{\delta_k^{SAR}=0}^{\delta_k^{SAR}=\delta_k^{opt}} p(\delta_k^{SAR}|\overline{C}). \tag{13}$$

$P(C|C)$ is the probability that a change was detected given that a change was present (percentage change correctly detected), $P(C|\overline{C})$ is the probability that a change was detected given that no change was present (percentage false alarms), $P(\overline{C}|C)$ is the probability that no change was detected given that a change was introduced and $P(\overline{C}|\overline{C})$ is the probability that no change was detected given that no change was introduced. The value of δ_k^{opt} is the decision threshold that minimizes the total Bayesian decision error. The results of the experiment is shown in figure 6. It is clear from this experiment that adding more than 23 autocorrelation lags (i.e $k = 23$) does not increase the performance of the method and consequently a k value of 23 was chosen. In [19], the autocorrelation summation as a means of making the TACD method more robust was also considered, in that study, which utilized MODIS time series data, it was also found that choosing a k parameter of 23 also gave optimal performance. From this, it is apparent that the TACD method using the lag summation strategy is robust across different datasets which reduces the requirement of utilizing training data to determine a specific k value for each region and dataset.

3.2.2. Selection of the δ^* parameter

As previously stated, there is a requirement that the method should produce a false alarm rate of $\leq 1\%$. This is due to the fact that the change algorithm is run over large areas and the validation of a large number of false alarms could be very costly and time consuming. To determine the threshold value that would yield a false alarm rate in this range, the Bayesian decision error was evaluated based on the distribution of the inferred change index (δ^{SAR}) using a training no-change dataset as follows

$$P(C|\overline{C}) = \int_{\delta_k^{SAR}=\delta_k^*}^{\delta_\tau^b=\infty} p(\delta^{SAR}|\overline{C}) = 0.01, \tag{14}$$

where δ_k^* is the decision threshold value and $P(C|\overline{C})$ is the false alarm rate. It can be seen from (14) that only no-change examples are required to determine the threshold value δ_k^*.

3.3. Bi-temporal SAR change detection

To justify the use of a stack of SAR imagery which is required for the hyper-temporal approach proposed in this paper, as opposed to having only two SAR images pre and post the change event, the proposed method was

Table 2: k , δ^{*}, $\delta^{\mathrm{LR}*}$ and False Alarm Rate (FAR) values

Method	k	δ^{*}	$\delta^{\mathrm{LR}*}$	FAR
SAR TACD	23	1.69	-	1%
Bi-temporal CD	-	-	0.996	1%

compared to a pixel based bi-temporal change detection formulation using only two images, one at the start and one at the end of the available SAR image stack. The most common operator in bi-temporal SAR change detection is the ratio operator [20], and in particular, we used the log-ratio operator as it has been shown to be very effective when considering change detection between SAR images [17, 18]. The change metric based on the log-ratio between SAR images was computed as

$$\delta_{i,j}^{\mathrm{LR}} = log\left(\frac{X_{t2}^{i,j}}{X_{t1}^{i,j}}\right), \tag{15}$$

where $\delta_{i,j}^{\mathrm{LR}}$ is the log ratio change metric at pixel (i, j). $X_{t1}^{i,j}$ is the SAR backscatter value for pixel (i, j) at time $t1$ (prior to the change event) with $X_{t2}^{i,j}$ being the SAR backscatter value for pixel (i, j) at time $t2$ (after to the change event). The change and no-change decision was then made using the following rule

$$\text{Change} = \begin{cases} \text{true} & \text{if } \delta^{\mathrm{LR}} \geq \delta^{\mathrm{LR}*} \\ \text{false} & \text{if } \delta^{\mathrm{LR}} < \delta^{\mathrm{LR}*}, \end{cases} \tag{16}$$

with $\delta^{\mathrm{LR}*}$ being the threshold value.

3.3.1. Selection of the $\delta^{\mathrm{LR}*}$ parameter

Similar to the approach used in section 3.2.2, the threshold value was selected to produce a false alarm rate of $\leq 1\%$. This was done by firstly calculating the change index value δ^{LR} using the training no-change dataset and calculating the corresponding threshold value as

$$P(C|\overline{C}) = \int_{\delta^{\mathrm{LR}}=\delta^{\mathrm{LR}*}}^{\delta^{\mathrm{LR}}=\infty} p(\delta^{\mathrm{LR}}|\overline{C}) = 0.01, \tag{17}$$

Table 3: Change Detection Accuracy (CDA) and False Alarm Rate (FAR) for both methods using parameters defined in sections 3.2.1 and 3.2.2

Method	CDA	FAR
SAR TACD	87%	0.8%
Bi-temporal CD	70%	1.6%

A summary of the selected parameters are given in table 2.

4. Results

4.1. SAR TACD performance on unseen dataset

Using the k and δ_k^* values determined in section 3.2.1, change was declared on a per pixel basis as follows

$$\text{Change} = \begin{cases} \text{true} & \text{if } \sum_{\tau=1}^{23} R(\tau, x, y) \geq 1.69 \\ \text{false} & \text{if } \sum_{\tau=1}^{23} R(\tau, x, y) < 1.69 \end{cases}$$

with the results shown in table 3. It can be seen that there is a strong correlation in the false alarm rate between the training and unseen datasets with the false alarm rate of the unseen dataset being within 0.2% of that of the training dataset. The change detection accuracy that was achieved was 87%.

4.2. Bi-temporal SAR change detection performance on unseen dataset

Using the $\delta^{\text{LR}*}$ value determined in section 3.3.1, change was declared on a per pixel basis using only the first and last SAR image in the time-series as follows

$$\text{Change} = \begin{cases} \text{true} & \text{if } \delta^{\text{LR}} \geq 0.996 \\ \text{false} & \text{if } \delta^{\text{LR}} < 0.996 \end{cases} \tag{18}$$

The results is also shown in table 3. It can be seen that similar to the SAR-TACD case, there is a once again a strong correlation in the false alarm rate between the training and unseen datasets with the false alarm rate of the unseen dataset in this case being within 0.6% of that of the training dataset.

The change detection accuracy that was achieved using the Bi-temporal CD method was 70%.

5. Discussion

From sections 3.3 and 4 it is clear that the proposed SAR-TACD method requires SAR time-series data as input as well as a no-change training dataset to determine a threshold value. The training dataset requirement is thus limited to only no-change examples which are numerous and can be obtained in large numbers as opposed to change examples that are rare at a regional scale [6]. Another attractive feature of the method is the fact that the k parameter has been shown to be very stable over multiple datasets which requires the operator to only set the the value of δ^* using a no-change dataset. It was found that there was a good correlation between the false alarm rate of the training (1%) versus the unseen datasets (0.8%) which implies a that the in-sample and out-of-sample errors based on the value of δ^* was roughly similar indicating good generalization of the method. The low false alarm rate of $\leq 1\%$ with a change detection accuracy of 87% makes the method attractive as a regional change alarm. As comparison, a bi-temporal change detection approach was also used using two images, one in the start of the SAR image stack and one at the end. The resulting change detection accuracy for the bi-temporal change detection method was 70%, which is 17% lower than that of the SAR-TACD method. The SAR-TACD method also compared well against a hyper-temporal optical change alarm framework proposed in [3] where the same study area was considered and a hyper-temporal optical time-series was used as input to a change alarm. The particular dataset that was used was the MODIS MCD43A4 data product. An overall accuracy of 88% was reported for the study area [3], whereas the SAR-TACD achieved an overall accuracy of 93%. Another advantage of the SAR-TACD method is when considering that speckle, which potentially has a significant impact in the case of image to image (bi-temporal) settlement detection due to the fact that the change in backscatter between the same pixel in two images due to speckle can be falsely seen as change. The advantage of the SAR-TACD approach is that because a time-series is used, speckle causes a local variation in the time-series but will not influence the backscatter trend. This can be clearly seen in figure 5 (left) where even in the case of the no-change time-series, significant local variation do occur but the time series mean remains largely constant. This is very different to the change time-series in figure 5

(right) where a definite trend is visible.

6. Conclusion

In this paper, the use of hyper-temporal SAR data for the detection of new informal settlements in the Gauteng province of South Africa was considered. A method previously shown to have good change detection performance using optical hyper-temporal time-series, the Temporal Autocorrelation Change detection (TACD) method [3], was extended an modified to work with hyper-temporal SAR data (SAR-TACD). This new change detection framework is intended to be used as a tool to alert operators to areas of possible changes between two dates which could then be validated using a secondary step (such as the use of high resolution imagery). As the algorithm is intended to be run over potentially very large areas (regional scale), a primary objective was to ensure that a very low false alarm rate should be maintained. It was shown that using new proposed SAR-TACD framework had a change detection accuracy of 87% when considering the detection of new or expanding settlements in the study area with a corresponding false alarm rate of $\leq 1\%$. It was also shown that the TACD method, which was originally applied to optical time-series data, was easily adapted for the use of SAR data and that certain parameters of the method (such as the k parameter) was found to be universal across data types, making the TACD approach very generic. Although specific change date information is not provided by the method, this algorithm could still be used effectively to determine areas of high change probability between two dates. An example would be mapping agencies wanting to identify areas of high change likelihood between mapping intervals. Although the SAR-TACD algorithm has only been tested for the case of new or expanding settlement detection in Gauteng, the method can easily be applied regionally. With the increase in the availability of historic (example ENVISAT ASAR) as well as future (example Sentinel-1) data holdings, the feasibility of using a SAR time-series based change detection approach is becoming increasingly more attractive.

[1] P. Snoeij, E. Attema, M. Davidson, B. Duesmann, N. Floury, G. Levrini, B. Rommen, B. Rosich, Sentinel-1 radar mission: Status and performance, Aerospace and Electronic Systems Magazine, IEEE 25 (8) (2010) 32–39. doi:10.1109/MAES.2010.5552610.

[2] A. Wiesmann, U. Wegmuller, T. Le Toan, M. Santoro, C. Werner, T. Strozzi, Use of envisat asar wide-swath mode data over siberia for large area land cover mapping, parameter retrieval, and change detection, in: Geoscience and Remote Sensing Symposium, 2005. IGARSS '05. Proceedings. 2005 IEEE International, Vol. 5, 2005, pp. 3595–3598. doi:10.1109/IGARSS.2005.1526625.

[3] W. Kleynhans, B. Salmon, J. Olivier, F. van den Bergh, K. Wessels, T. Grobler, K. Steenkamp, Land cover change detection using autocorrelation analysis on modis time-series data: Detection of new human settlements in the gauteng province of south africa, Selected Topics in Applied Earth Observations and Remote Sensing, IEEE Journal of 5 (3) (2012) 777 –783. doi:10.1109/JSTARS.2012.2187177.

[4] R. Mitchell, Change-driven mapping, Geospatial Intelligence Forum 10 (4) (2012) 22–24.

[5] J. Verbesselt, R. Hyndman, G. Newnham, D. Culvenor, Detecting trend and seasonal changes in satellite image time series, Remote Sensing of Environment 114 (1) (2010) 106–115.

[6] R. S. Lunetta, J. F. Knight, J. Ediriwickrema, J. G. Lyon, L. D. Worthy, Land-cover change detection using multi-temporal MODIS NDVI data, Remote Sensing of Environment 105 (2) (2006) 142–154.

[7] K. de Beurs, G. Henerby, A statistical framework for the analysis of long image time series, International Journal of Remote Sensing 26 (8) (2005) 1551–1573.

[8] R. Kennedy, W. Cohen, T. Schroeder, Trajectory-based change detection for automated characterization of forest disturbance dynamics, Remote Sensing of Environment 110 (3) (2007) 370–386.

[9] B. Salmon, J. Olivier, W. Kleynhans, K. Wessels, F. van den Bergh, K. Steenkamp, The use of a multilayer perceptron for detecting new

human settlements from a time series of modis images, International Journal of Applied Earth Observation and Geoinformation 13 (6) (2011) 873–883.

[10] W. Kleynhans, J. C. Olivier, K. J. Wessels, B. P. Salmon, F. van den Bergh, K. Steenkamp, Detecting land cover change using an extended kalman filter on MODIS NDVI time-series data, IEEE Geoscience and Remote Sensing Letters 8 (3) (2011) 507–511.

[11] T. Grobler, E. Ackermann, A. van Zyl, J. Olivier, W. Kleynhans, B. Salmon, Using Page's cumulative sum test on modis time series to detect land-cover changes, IEEE Geoscience and Remote Sensing Letters 10 (2) (2013) 332–336.

[12] W. Kleynhans, J. C. Olivier, K. J. Wessels, B. P. Salmon, F. van den Bergh, K. Steenkamp, Improving land cover class separation using an extended Kalman filter on MODIS NDVI time series data, IEEE Geoscience and Remote Sensing Letters 7 (2) (2010) 381–385.

[13] F. Henderson, Z.-G. Xia, SAR applications in human settlement detection, population estimation and urban land use pattern analysis: a status report, Geoscience and Remote Sensing, IEEE Transactions on 35 (1) (1997) 79–85. doi:10.1109/36.551936.

[14] P. Gamba, G. Lisini, Fast and efficient urban extent extraction using ASAR wide swath mode data, Selected Topics in Applied Earth Observations and Remote Sensing, IEEE Journal of 6 (5) (2013) 2184–2195. doi:10.1109/JSTARS.2012.2235410.

[15] M. Marghany, Fuzzy b-spline optimization for urban slum three-dimensional reconstruction using envisat satellite data, in: IOP Conference Series: Earth and Environmental Science, Vol. 20, IOPscience, 2014, pp. 1–7.

[16] M. Marghany, Hologram interferometric sar and optical data for fourth-dimensional urban slum reconstruction, in: Asian Conference on Remote Sensing, Vol. 35, 2014.

[17] L. B. Y. Bazi, F. Melgani, An unsupervised approach based on the generalized gaussian model to automatic change detection in multitemporal

sar images, IEEE Transactions on Geoscience and Remote Sensing 43 (4) (2005) 874–887.

[18] C. Carincotte, S. Derrode, S. Bourennane, Unsupervised change detection on sar images using fuzzy hidden markov chains, IEEE Transactions on Geoscience and Remote Sensing 44 (2) (2006) 432–441.

[19] W. Kleynhans, Salmon, K. Wessels, A spatio-temporal autocorrelation change detection approach using hyper-temporal satellite data, in: Geoscience and Remote Sensing Symposium (IGARSS), 2013 IEEE International, 2013, pp. 6765 –6768.

[20] E. Rignot, J. V. Zyl, Change detection techniques for ERS-1 SAR data, IEEE Transactions on Geoscience and Remote Sensing 31 (4) (1993) 896–906.

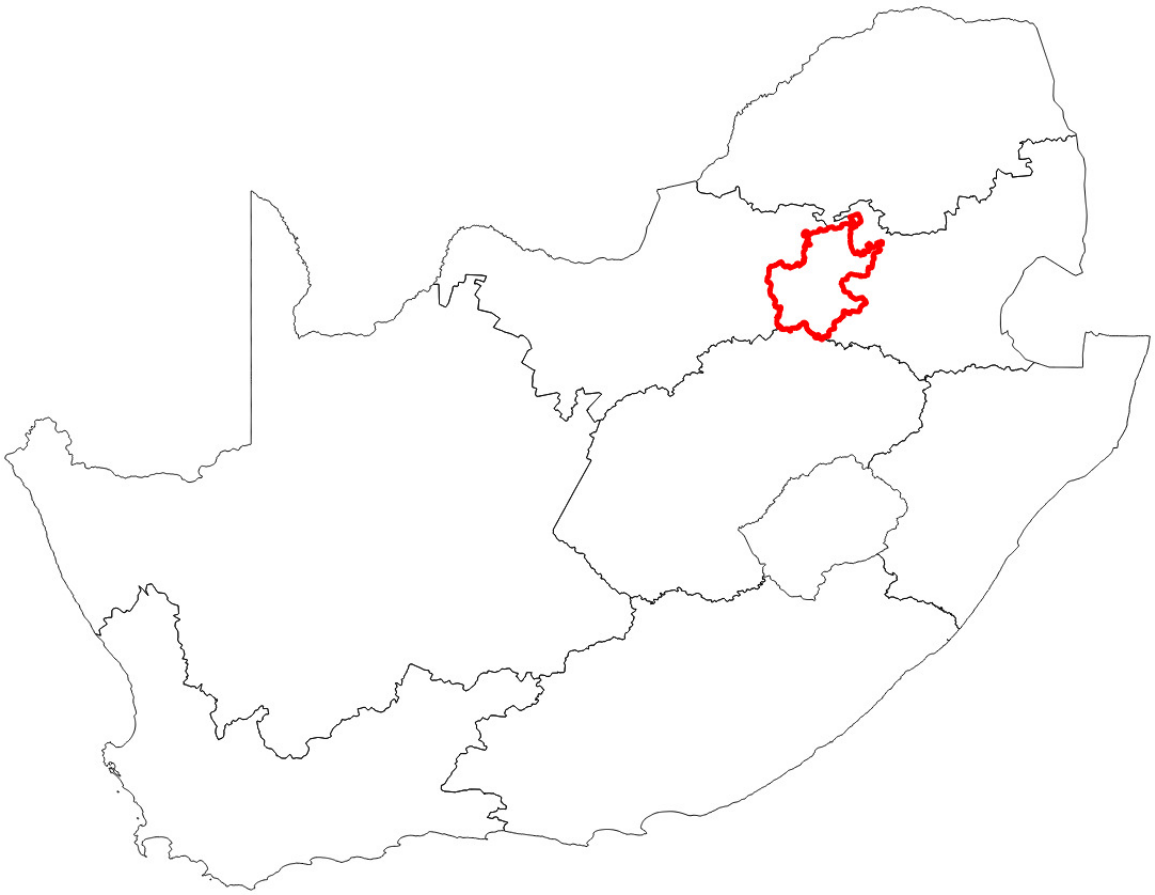

Figure 1: The study area used in this study was the Gauteng province (red outline) located in the north-central part of South Africa.

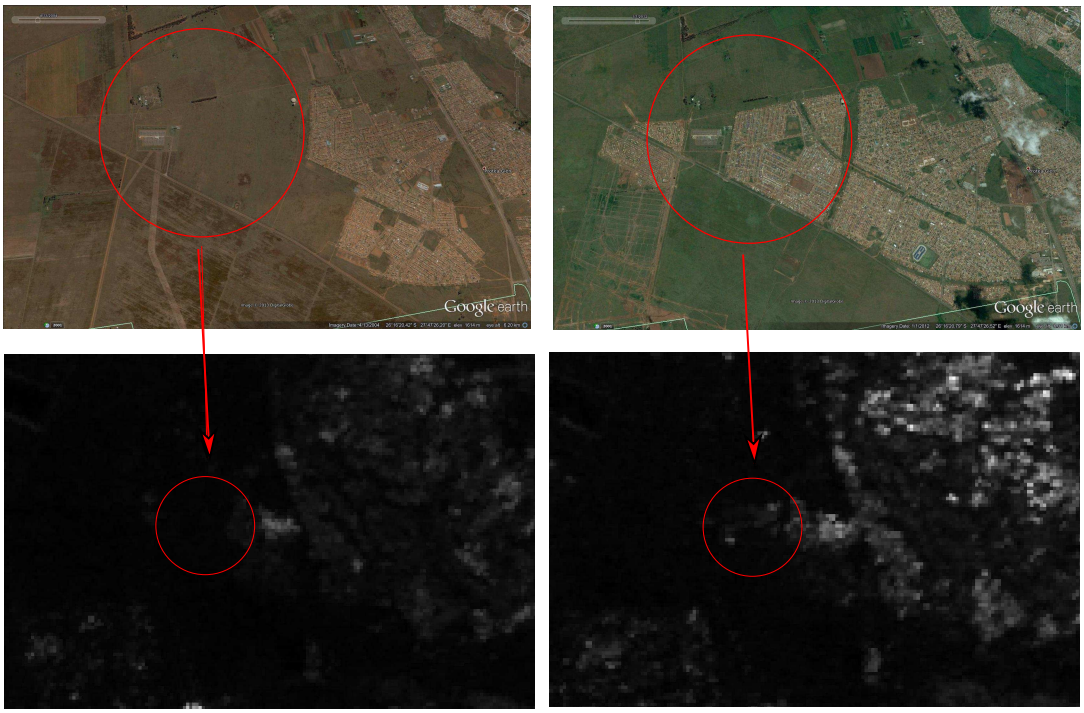

Figure 2: Example of a new settlement development that formed between 2005 and 2011. Quickbird image on the top left shows the area in 2005 being mostly covered by natural vegetation whereas the Quickbird image on the top right shows a new settlement that was formed (Images courtesy of Google earth^{TM}). The corresponding no-change area is also indicated on an ASAR WSM image shown respectively on the bottom left and right.

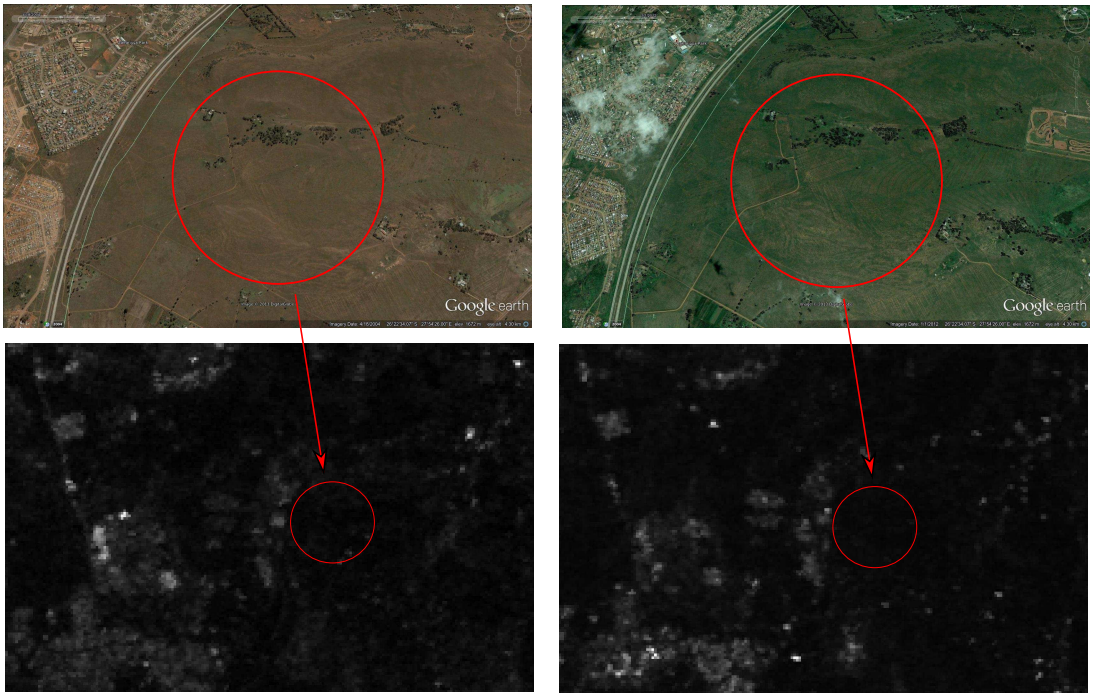

Figure 3: Example of an area that was mostly unchanged between 2005 and 2011. Quickbird image on the left shows the area in 2005 being mostly covered by natural vegetation where the Quickbird image on the right shows the same area remaining unchanged (Images courtesy of Google earth^{TM}).The corresponding change area is also indicated on an ASAR WSM image shown respectively on the bottom left and right.

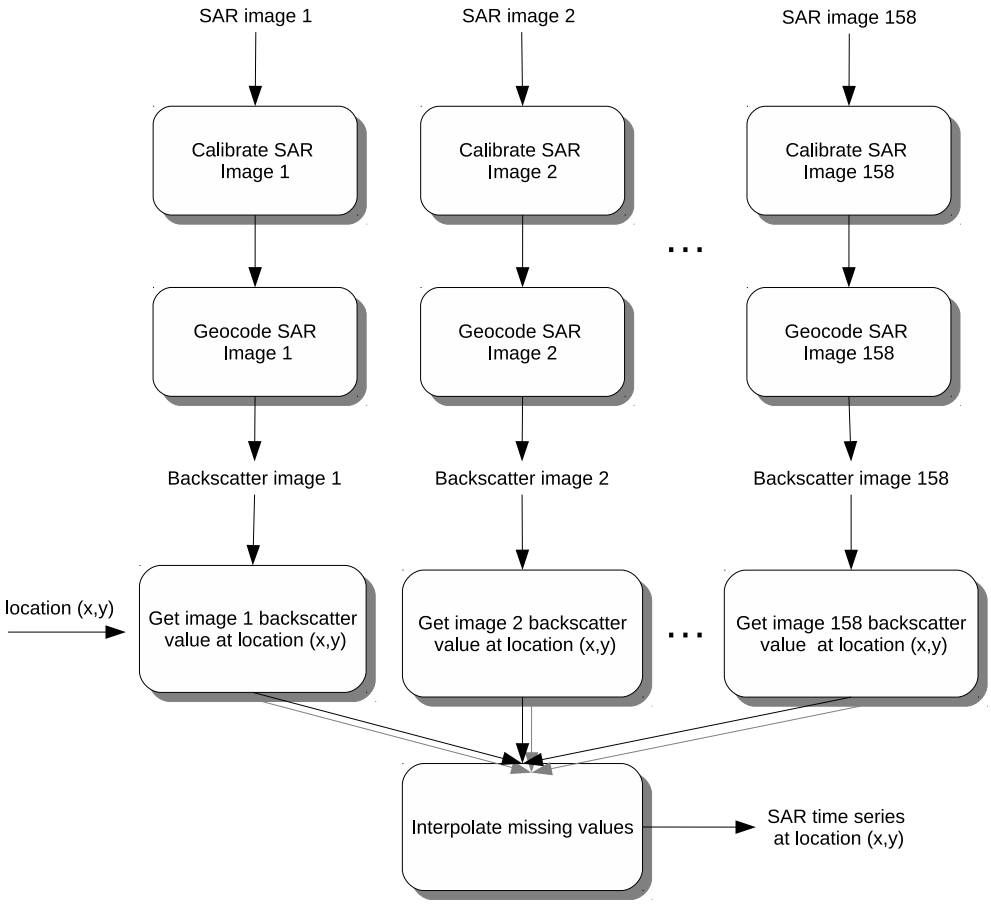

Figure 4: Flow diagram showing how a pixel time series was generated for a specific location (x,y) using the ASAR image stack.

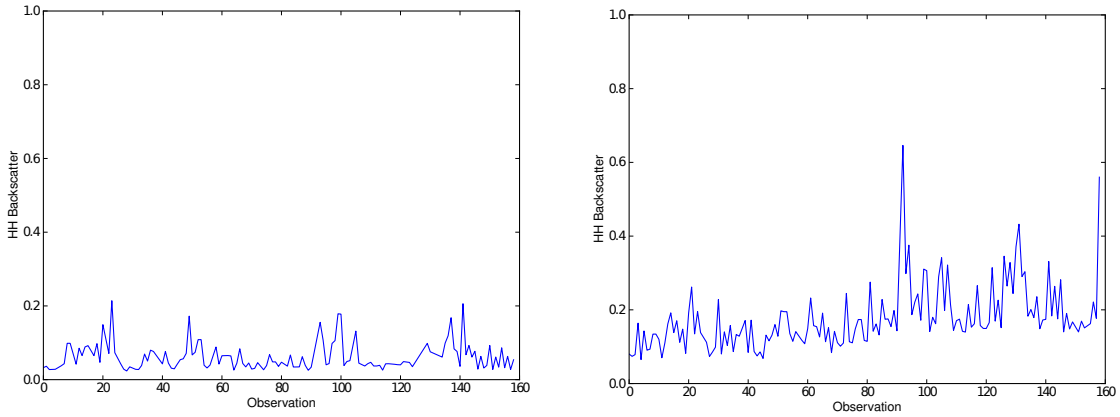

Figure 5: Hyper temporal SAR HH backscatter time-series between 2005 and 2011 for a ASAR WSM pixel corresponding to a change (right) and no-change (left) area respectively.

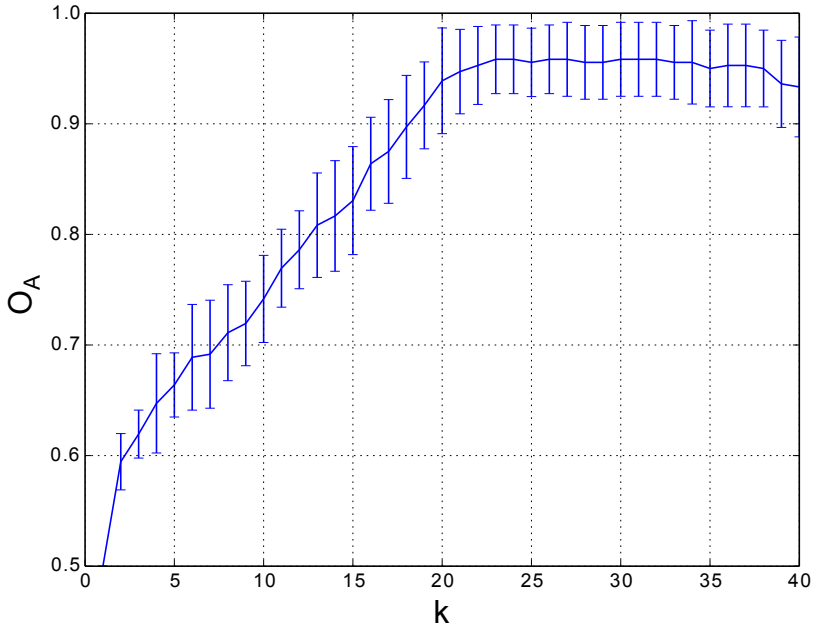

Figure 6: Overall Accuracy (O_A) as a function of the value of k with the standard deviation at each k value shown as an error bar. It can be seen that increasing the value of $k = 23$ does not increase O_A.